Processing of functional fine scale ceramic structures by ink-jet printing

M. Mougenot, Martine Lejeune, Rémy Boulesteix, B. Fousseret, Bernard Soulestin, Jean-François Baumard, C. Boissiere, Carmen Navarro Sanchez, D. Jalabert, C. Richard, et al.

J.G.Heinrich and C. Aneziris, Proc. 10th ECerS Conf., Göller Verlag, Baden-Baden, 2007, 476-481, ISBN: 3-87264-022-4

Processing of Functional Fine Scale Ceramic Structures by Ink-Jet Printing

M. Mougenot[1], M. Lejeune[1*], R. Boulesteix[1], B. Fousseret[1], B. Soulestin[1], J. F. Baumard[1], C. Boissiere[2], C. Sanchez[2], D. Jalabert[3], C. Richard[4], D. Audigier[4], R. Noguera[5], C. Dossou-Yovo[5]

[1] Ecole Nationale Supérieure de Céramique Industrielle, Laboratoire Science des Procédés Céramiques et de Traitements de Surface, Limoges, France
[2] Laboratoire de Chimie de la Matière Condensée, UPMC, Paris, France
[3] Centre de Microscopie Electronique, Université d'Orléans, Orléans, France
[4] Laboratoire de Génie Electrique et de Ferroélectricité, INSA Lyon, France
[5] CERADROP, Limoges, France

Abstract

This review illustrates the potentiality of ink-jet printing for the fabrication of functional fine scale ceramic structures corresponding to two different kinds of micro-pillar arrays i.e. (i) PZT skeletons for 1-3 piezoelectric ceramic polymer composites or (ii) structures of functionalised mesoporous silica microdots. The functional properties of the corresponding structures will be also reported.
Keywords : Printing, Suspensions, PZT, Silica, Mesoporous, Hydrophobicity.

Introduction

Ink-jet printing process has been recently explored as a solid freeforming fabrication (SFF) technique to produce 3D ceramic parts [1-11]. The prototyping techniques developed up to now for ceramic parts such as stereolithography [12-16], fused deposition modeling [17,18] and selective laser sintering [19] are characterized by a definition of around 150µm, and do not allow to deposit different materials on the same layer. In comparison, ink-jet printing prototyping process opens the way to the development of multifunctional 3D fine scale ceramic parts.
Ink-jet printing prototyping process consists in depositing ceramic system micro-droplets (a few pl) ejected via nozzles to build the successive layers of the 3D structures. Consequently, by adjustment of the aperture of the printing head and the control of the spreading phenomenon of the droplet, one can expect to reach a standard definition of around 50µm and even ultimately of 10µm, taking into account the tremendous evolution in the printing field. Thanks to its high flexibility in terms of design because of its capability to deposit different materials with a high definition, this technique may be applied to the production of sophisticated microelectronic devices integrating metallic connection network (medical imaging probes, packaging, micro-actuators or sensors, ...).

In order to demonstrate the potentiality of the ink-jet printing for the fabrication of functional fine scale ceramic parts by ink-jet printing, our investigations have been focused on the case of micro-pillar array structures for different applications such as:

(i) PZT skeletons, which once embedded in polymer, can be used as 1-3 piezoelectric ceramic polymer composites for medical imaging probes.
Ink-jet printing process could lead to the evolution of medical imaging probes in terms of performances thanks to the improvement of their spatial resolution by generating very fine scale ceramic structures on the one hand, and of their configuration by variable size, shape and distribution of ceramic rods inside the probes on the other hand,
(ii) mesoporous silica microdots which can be used as multifunctional sensors.
In the last decade, extensive work has been reported on the fabrication of mesoporous silica films by Evaporation-Induced Self-Assembly (EISA) *i.e* by evaporation of a solution of polymerisable inorganic precursors and surfactant molecules [20-25]. In this case, one can initiate the self-assembly of surfactant micelles within the inorganic precursors to yield an organized hybrid mesostructure. These well organized mesoporous structures, with mesopores dimensions ranging from 2nm to 20nm, can be functionalised by *in-situ* grafting during the EISA process.
Recent papers [26-28] have reported the feasibility of patterned self-assembly monolayers by combining silica-surfactant self-assembly with three processing routes (pen lithography, ink-jet printing and dip-coating). In fact, by coupling ink-jet printing process and evaporation-induced self assembly (EISA), microdots arrays of functionalized mesoporous silica could be achieved. Moreover, by using a multinozzle system, one can expect to generate multifunctional mesoporous micro-dots arrays by variation of the functionalisation from one dot to another, thanks to *in-situ* grafting occurring during the EISA process.

Experimental

Fabrication of micro-pillar arrays

The main technical characteristics of the ink-jet printing equipment are as follows: the printing equipment is a drop-on-demand one with multi-nozzle piezoelectric printing heads (52 µm aperture). The nozzles can be electrically driven independently or simultaneously. The printing head displacement has a resolution of 0.5µm, a reproducibility of 2µm and an accuracy of 2µm.

Additional technical data are given in the corresponding patent (PCT/RF04/02150), and by the equipment manufacturer under the reference Ceraprinter L01 [Ceradrop, Ester Technopole, BP 6935, Limoges (France)].

Before fabrication, the electric pulse applied to the nozzle was adjusted for each fluid to have a consistent droplet ejection. This step was carried out by capturing stroboscopically backlit images of the ejection with a CCD camera. By this way, the velocity and the size of the droplet during ejection and before spreading were controlled as a function of the driving parameters of the printing head. Previous works [29] revealed that the final droplet velocity and volume, i.e. the droplet kinetic energy, increase with the amplitude of the pulse.

The micro-pillar arrays were obtained through successive deposition steps of droplets periodically spaced out. The effect of the time gap (drying time) between the successive layers on the characteristics of the micro-pillar arrays was studied.

The PZT micro-pillar arrays were deposited at room temperature on green sheets obtained by tape casting of organic PZT suspensions. The mesoporous silica microdots were deposited at room temperature by ink-jet printing the silica sols on hydrophilic silicon wafers with hydroxylated native silicon oxide.

Adjustement of the fluid properties

To enable ink jet printing, the fluids must have a viscosity and a surface tension ranging between 5 and 20 mPa.s and between 30 and 35mN/m respectively, which corresponds to the specifications of the jetting fluid given by the printing-head supplier. In addition, to obtain droplet generation, a ratio of ejection $Re/We^{1/2}$ in the adequate range (1-10), is required to minimize pressure for ejection and avoid satellite droplet formation. Reynolds number (Re) by Weber number (We) ratio equals $(\sigma\rho r)^{1/2}/\eta$, where Re equals $v.r.\rho/\eta$, We equals $v^2.r.\rho/\sigma$ and ρ, η and σ are the ink density, viscosity and surface tension respectively, r the radius of the nozzle and v the fluid velocity. A low vapor pressure of the solvents is needed to avoid too rapid evaporation at the nozzle aperture.

1) Characteristics of the PZT suspensions

Different investigations were carried out to adjust the PZT suspensions formulation in terms of the nature, the content of the different organic compounds (solvent, dispersant, binder…) and the ceramic loading to be compatible with the ink-jet printing process, not only in regards to the fluid properties mentioned previously but also to avoid sedimentation, premature drying of the ink within the nozzle, to prevent the clogging of the printing-head. Moreover, the formulation of the ceramic suspensions was also chosen taking into account the optimal characteristics of the deposit for each layer, i.e (i) high green compacity, (ii) large and homogeneous thickness, (iii) high definition and (iv) high green mechanical strength. These aspects will be underlined later.

At first, water was selected as solvent for the ceramic PZT suspensions to combine a slow evaporation with environmental benefits. Moreover, for ceramic suspensions, the particle size distribution of the powder must be adjusted to obtain a ratio of 50 between the nozzle aperture and the maximum diameter of the powder, to avoid the blocking of the nozzle. Consequently, as the aperture of the printing head is 52 µm, the maximum diameter of the PZT powder was adjusted by attrition milling to 1µm.

The content of dispersant was adjusted to reach a minimum viscosity at the end of the milling step of the PZT powder corresponding to a high ceramic loading (around 40vol%) to guarantee the stability of the ceramic suspension in the reservoir of the ink-jet printing equipment.

After milling, the PZT suspensions was diluted to avoid the blocking of the nozzles and a high molecular weight binder was added to increase the viscosity . By this way, the appropriate viscosity of the suspension (i.e. 10mPa.s) was reached for a 15 vol% PZT loaded suspensions with a high PZT/(PZT+binder) vol%, i.e 75%. This suspension exhibits a Newtonian behavior and was characterized by surface tension around 59mN/m. The surface tension of the ink was adjusted to an appropriate value of 30mN/m by addition of a surfactant.

2) Characteristics of the silica sols

The precursor solutions were based on chemical compositions developed for the deposition of mesoporous silica films by dip-coating [20-25] i.e. :

- tetraethylorthosilicate (TEOS) was used as polymerisable inorganic precursor,
- pH was adjusted to 1.85 by addition of nitric acid to water with a H_2O/Si molar ratio fixed at 5, to favor fast hydrolysis and minimum condensation promoting the formation of small oligomers,
- the triblock copolymer Pluronic F127 (PEO_{106}-PPO_{70}-PEO_{106}) was used as non-ionic surfactant. In fact, the large molecular weight of the F127 allows to reach an appropriate viscosity (i.e. 4.8 mPa.s) for a F127/TEOS molar ratio equal to 0.006 and an EtOH/TEOS molar ratio of 20.

Moreover, the addition of hydrophobic organosilane cosurfactant R'-$Si(OR)_3$ *i.e.* $F_3C(CF_2)_5CH_2CH_2Si(OC_2H_5)_3$ (TFTS) to the F127 formulation was also investigated with a TFTS/TEOS molar ratio of 5%. Because of its hydrophobic character, TFTS addition could contribute to improve the deposit definition on hydrophilic substrates, to increase the hydrophobicity of the micro-dots arrays and to modify the silica-surfactant self-assembly.

The aging time of the corresponding solutions was adjusted to control the size of the oligomers in order to guarantee during the evaporation of the solvent, the self-assembly of the micelles with the organic precursor during the evaporation of the solvent and to avoid clogging of the printing head by formation of a gel. ^{29}Si NMR studies of TEOS hydrolysis for the F127 solution and with addition of TFTS have allowed to select different aging times corresponding to mainly Q_2 $[Si(OSi)_2(OX)_2]$ and Q_3 $[Si(OSi)_3(OX)]$ condensed species [30]. In fact, a small size of oligomers (mainly Q_1 $[Si(OSi)(OX)_3]$ species) inhibits the formation of a

silica inorganic network whereas a high degree of condensation (mainly Q_4 [$Si(OSi)_4$] species) prevents the organization of the surfactant from occuring. Therefore, for F127 solution, the aging time was fixed to 96h (4 days). As an increase in condensation rate is observed after addition of 5mol% TFTS, different solutions were prepared before ejection with aging times corresponding to 48h or 96h.

Results and Discussion

Characteristics of the PZT micro-pillar arrays

1) Microstructural characterization of the green and sintered micro-pillar arrays

The configuration of the PZT micro-pillar arrays is adjusted in order to obtain final ceramic polymer piezoelectric composites with a volume fraction of PZT in the range 30 - 33 vol %. In fact, this range is determined by a compromise to achieve a high piezoelectric charge coefficient (d_{33}) and, at the same time, a moderate acoustic impedance (Z) and a high thickness coupling coefficient (k_t) [31].

Figure 1 illustrates one pillar of the green arrays obtained by successive depositions of droplets via a multi-nozzle printing-head (200 layers with 4s drying time between two successive layers). This one is characterized by :

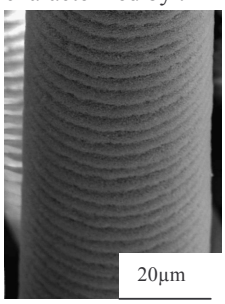

-a mean diameter around 45µm. Compared to the 52µm nozzle aperture, this high definition could result from the coalescence of the particles during the drying after droplet impact.

-A very good stacking of the different layers with a growth rate equal to 6µm/layer .

Fig.1 SEM image of one green ink-jet printed PZT pillar.

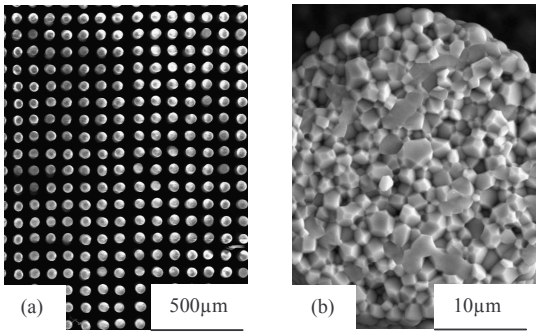

Fig. 2 (a) SEM image of a sintered PZT micro-pillar array (200 layers) (b) Cross-section of one sintered PZT micro-pillar.

Once the conditions of fabrication of large PZT micro-pillar arrays were optimized as shown just before, different trials were performed to adjust the conditions of sintering. A specific PbO sintering atmosphere was used to guarantee the stoechiometry of the sintered material, taking into account the high corresponding developed surface of the structure. After sintering at 1250°C, very dense pillars were obtained characterized by a mean diameter of 38µm (Fig. 2), which corresponds to a shrinkage of 15%.

2) Piezoelectric properties of the 1-3 piezoelectric ceramic polymer composites

The different sintered PZT skeletons were then embedded in a polymer matrix and the thickness of the composite was adjusted to 600µm or 130µm to define variable thickness resonant frequency (*f*) as this one is inversely proportional to the thickness of the transducer (*t*) according to the equation:

$f=v/2t$ where v is the velocity of the sound in the composite transducer.

Table I shows the dielectric and electromechanical properties measured for the different ceramic polymer composites made by ink-jet printing (IJP) and compared to the one of commercial 1-3 ceramic polymer composites using dice and fill technique (DF) with the same PZT material.

	IJP composites		DF composites
Volume fraction of PZT (%)	33	30	25-30
Pitch a(µm)	61	66	-
Thickness t (µm)	600	130	>600
t/a	10	2	-
ε_r	630	650	525
tg δ (%)	3	4	3
k_t (%)	55	46	50-70
f(MHz)	3	12	0.15-1.5
ν =f*2t (m/s)	3600	2880	-
ρ (kg/m^3)	3260	3060	-
Z=ρ*ν (Mrayl)	11.73	8.81	-

Table I Dielectric and electromechanical properties of Ink-Jet Printing (IJP) and Dice and Fill (DF) composites.

The IJP and DF composites showed similar properties as dielectric and electromechanical characteristics are concerned, which shows that IJP is a reliable process to fabricate polymer ceramic piezoelectric composites. Moreover, fine scale structures can be achieved by IJP technique (38µm pillar diameter) which allows to develop very high frequency transducers (> 10MHz) and consequently to improve the spatial resolution of the ultrasonic medical probes. In fact, to avoid lateral resonance (lamb waves), the thickness must be much larger than the pitch a corresponding to the spacing between the pillars centers, which means that the pillar diameter must decreases as the frequency increases.

Therefore, in the future, one can expect to still improve the acoustic properties of the high frequency (>10MHz) IJP composites by decreasing the size of the pillar which would allow to increase the ratio t/a and guarantee a pure thickness resonance mode.

Characteristics of the mesoporous silica micro-dots arrays

Previous studies [32,33] have identified the different steps of structural organization of a F127 based film from the sol: (I) spherical then cylindrical micelles first form upon evaporation then , (II) a few ten of seconds

after deposition, cylindrical micelles self-organize into random oriented 2D hexagonal domains, and finally, (III) after few min when the evaporation is considered to be done, the silica phase is still flexible enough to allow the domains close to the interfaces to realign with these one with propagation of this orientation from the interfaces to the center of the film. But in parallel, the silica matrix undergoes further condensation leading to the rigidification of the inorganic network. So, realignment and condensation are in competition. Consequently, if the film is too thick or the initial sol too highly condensed, a randomly orientated phase of domains remains at the film center between both well-aligned interfacial phases.

Therefore, in the case of patterned dots arrays, the influence of different parameters were studied in regards to the mesostructure organization i.e the aging time of the sol, the number of stacked layers and the drying time between two successive layers.

Before characterization, the different patterned arrays were heated at 130°C for 2 days to stiffen the inorganic network through extended condensation.

1) Characterization of the Structural Organization of monolayer microdots arrays

GISAXS characterizations of monolayer microdots arrays of F127 formulations with or without TFTS reveals that the mesostructure organization is improved by addition of 5mol% TFTS. In fact, sharp diffraction spots are observed for monolayer microdots arrays using TFTS formulations (Fig. 3b) which indicates a preferential orientation of organized domains parallel to the substrate, whereas a diffraction ring is observed for monolayer microdots arrays using F127 formulations without TFTS (Fig. 3a) which can be attributed to domains that have random orientations with respect to the surface.

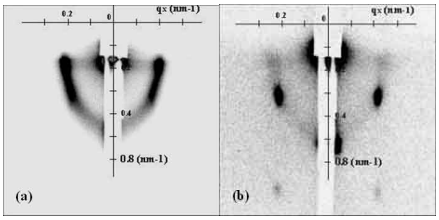

Fig.3 2D-SAXS patterns of monolayer microdots arrays deposited by ink-jet printing of F127 solutions (a) and with 5mol% TFTS addition (b) for 96h aging time.

For 5mol% TFTS formulations, the alignment of cylindrical pores parallel to the interfaces is confirmed by transmission electronic microscopy observations (Fig. 4): each monolayer microdot exhibits, in its whole thickness (350nm), a structural organization corresponding to a centered rectangular structure with cylindrical micelles parallel to the interfaces. This structure results from the shrinkage of a 2D hexagonal arrangement of the micellar cylinders in a direction perpendicular to the interfaces during the thermal treatment of the deposits at 130°C as mentioned in previous work [34].

Addition of an hydrophobic organosilane such as TFTS could act as a co-surfactant, once hydrolyzed, promoting the co-assembly of the surfactant and silica species (step I) by interaction of its hydrophobic group with the hydrophobic blocks PO of F127.

Consequently, this leaves more time for the steps II and III before the complete rigidification (condensation) of the silica network which can explain the beneficial effect of TFTS in regards to the mesostructure organization of the monolayer deposits.

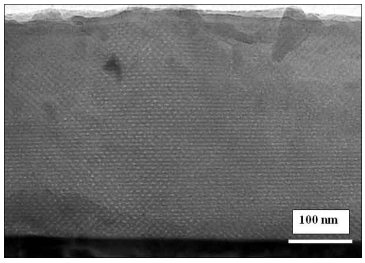

Fig.4 TEM micrograph of a cross-sectioned monolayer microdot made with the 5mol% TFTS solution.

2) Characterization of the Structural Organization of multilayer microdots arrays

a) Effect of the drying time between two successive layers

X-Ray diffraction (XRD) characterizations of the multilayer microdots arrays in θ-2θ Bragg-Brentano scattering geometry reveal that the mesostructure organization of multilayer deposits of TFTS formulation sols is improved by increasing the drying time between two successive layers (Fig. 5)

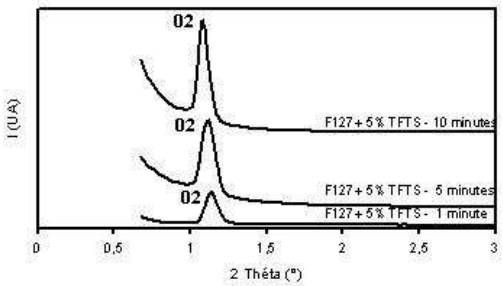

Fig.5 1D X-Ray diffraction of a 5 layers microdots arrays made with the 5mol% TFTS solution for different drying times between two successive layers (aging time: 96h)

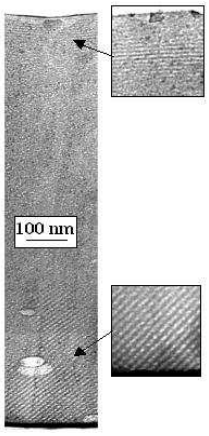

For a short drying time (1min), MET observations of multilayer deposits (5 layers) have revealed that only the interfaces exhibit a mesostructure organization (Fig. 6). In fact, because of the very short time between two successive deposits, one single droplet is formed and the mesostructure organization occurs only close to the interfaces due to the too high thickness of the global deposit.

Fig.6 TEM micrograph of a cross-sectioned 5 layers microdot made with the 5mol% TFTS solution for a drying time of 1min between two successive layers (aging time: 96h)

For a longer drying time (10min), well organized domains are observed on a 1.5µm thickness (Fig. 7). As found for the monolayer deposits, the structural organization corresponds to a centered rectangular structure with cylindrical micelles parallel to the interfaces, with different orientations around the direction b. The rectangular cell parameters are a=14nm and b=12.6nm.

The bottom layers of the multilayer deposits exhibit a worm-like structure (Fig. 7) which could result from the degradation of the structural organization due to the accumulation of solvent, during the stacking of the successive layers.

Therefore, it appears that the increase of the drying time between two successive layers allows the structural organization of each deposited layers in its whole thickness, as revealed by the organization of the surface of the multilayer microdot on a significant thickness corresponding to around 3 layers. Moreover, the increase of the drying time between two successive layers contribute to limit the accumulation of the solvent and therefore the degradation of the structural organization of the bottom layers.

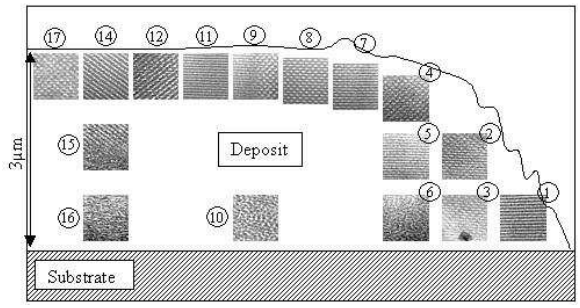

Fig.7 TEM micrograph of a cross-sectioned 5 layers microdot made with the 5mol% TFTS solution for a drying time of 10min between two successive layers (aging time: 96h).

b) Effect of the aging time of the sols

Figure 8 reveals that the mesostructure organization of multilayer microdots of TFTS formulation sols is improved by decreasing the aging time of the sols from 96h to 48h. As mentioned before, ^{29}Si NMR studies of TEOS hydrolysis for the F127 based solutions revealed an increase in condensation rate by addition of 5mol% TFTS. So by increasing the aging time of the sols from 48h to 96h, the realignment of the organized domains with the interfaces of the deposits can be limited by the too high condensation of the sols leading to a faster rigidification of the silica network.

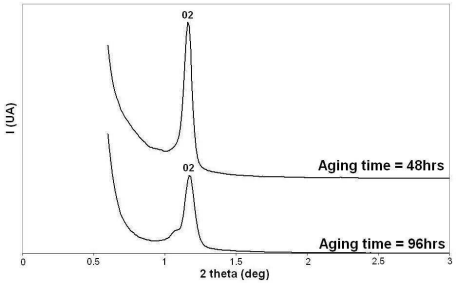

Fig.8 1D X-Ray diffraction of a 5 layers microdots arrays made with the 5mol% TFTS solution for different aging times (drying time: 10min)

c) Effect of the numbers of stacked layers

For the applications of micro-dots arrays as chemical sensor, a sufficient mesoporous volume must be reached in order that the adsorption could be detectable. One alternative is to increase the number of layers. Therefore, 25 layers deposits have been achieved by ink-jet printing TFTS formulations according to the conditions corresponding to the best structural organization, i.e with a 48h aging time of the sols and 10min drying time between successive layers.

Figure 9 shows a significant structural organization of the microdots arrays corresponding to the stacking of 25 layers. Characterizations of the corresponding accessible porous volume and pore size distribution are in progress.

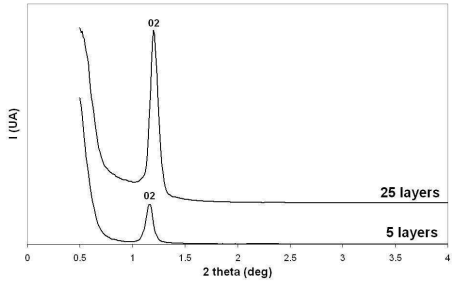

Fig.9 1D X-Ray diffraction of microdots arrays made with the 5mol% TFTS solution for different number of layers (aging time: 48h, drying time: 10min)

SEM images reveal well defined patterned arrays with microdots corresponding to domes, characterized by a diameter around 110µm and a mean height around 20µm (Fig. 10). This good definition of the patterned arrays can be correlated to the hydrophobic character of the TFTS limiting the wetting of the hydrophilic silicon wafers.

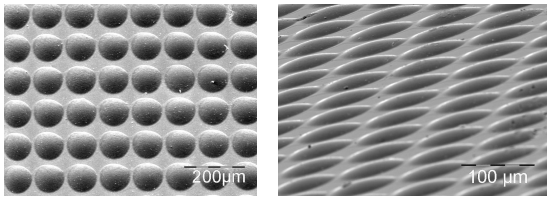

Fig.10 SEM images of 25 layers microdots arrays made with the 5mol% TFTS solution (aging time: 48h, drying time: 10min).

References

1. P. F. Blazdell, J. R. G. Evans, M. J. Edirisinghe, P. Shaw and M. J. Binstead. The computer aided manufacture of ceramics using multilayer jet printing. *J. Mat. Sci. Lett.* **14** (1995), 1562 - 1565.
2. M. Mott, J.H. S and J. R. G. Evans. Microengeneering of ceramics by direct ink-jet printing. *J. Am. Ceram. Soc.* **82** – 7 (1999), 1653-1658.
3. M. Mott and J. R. G. Evans. Zirconia/alumina functionally graded material made by ceramic ink-jet printing. *Mat. Sci. and Eng*. **A271** (1999), 344 - 352.
4. Q. F. Xiang, J. R. G. Evans, M. J. Edirisinghe and P. F. Blazdell. Solid freeforming of ceramics using a drop-on-demand jet printer. *Proc. Instn. Mech. Engrs* **211** part B (1997), 211 - 214.

5. N. Reis, K. A. M. Seerden, B. Derby, J. W. Halloran and J. R. G. Evans. Direct ink-jet deposition of ceramic green bodies I – II. *Mat. Res. Soc. Symp. Proc.* **542** (1999), 141 - 151.
6. N. Reis, K. A. M. Seerden, B. Derby, J. W. Halloran, J. R. G. Evans and P. S. Grant. Ink-jet printing of wax-based alumina suspension. *J. Am. Ceram. Soc*. **84** (2001), 2514-2520.
7. N. Reis, B. Derby and C. Ainsley. Freeform fabrication by controlled droplet deposition of powder filled melts. *J. Mat. Sci.* **37** (2002), 3155-3161.
8. A. R. Bhatti, M. Mott, J. R. G. Evans and M. J. Edirisinghe. PZT pillars for 1-3 composites prepared by ink-jet printing. *J. Mat. Sci. Lett*. **20** (2001), 1245 - 1248.
9. M. M. Moheb and J. R. G. Evans. A drop-on-demand ink-jet printer for combinatorial libraries and functionally graded ceramics. *J. Comb. Chem*. **4** (2002), 267-274.
10. W. D. Teng and M. J. Edirisinghe. Development of continuous direct ink jet printing of ceramics. *British Ceramic Transactions* **97**-4 (1998), 169-173.
11. X. Zhao, J. R. G. Evans, M. J. Edirisinghe and J. H. Song. Ink-jet printing of ceramic pillar arrays. *J. Mat. Sci***37**. (2002), 1987-1992.
12. A. Bertsch. Microstéréolithographie par masquage dynamique. Thèse de doctorat. Institut National Polytechnique de Lorraine, France, (1996).
13. C. Hinczewski, S. Corbel and T. Chartier. Ceramic suspensions suitable for stereolithography. *J. Eur. Ceram. Soc.* **18** (1998), 583.
14. F. Doreau, C. Chaput and T. Chartier. Stereolithography for manufacturing ceramic parts. *Advanced Engineering Materials*. **2** (8) (2000), 493
15. C. Hinczewski, S. Corbel and T. Chartier. Stereolithography for the fabrication of ceramic three-dimensional parts. *Rapid Prototyping J.* **4** (3) (1998), 104.
16. T. Chartier, C. Chaput, F. Doreau and M. Loiseau. Stereolithography of structural complex ceramic parts. *J. Mat. Sc.* **37**, (2002), 3141-3147.
17. Song et al. Development of metal-polymer composites for fused deposition modelling. *Proceedings of the 7th European Conference of Rapid Prototyping and manufacturing, Nottingham,* (1998)
18. Lous et al. Fabrication of piezoelectric ceramic/polymer composite transducers using fused deposition of ceramics. *J. Am. Ceram. Soc*. **83** – 1 (2000), 124 - 128.
19. Tolochko et al. Fabrication of micromechanical component by laser sintering of fine powders. *10th European Conference on Rapid Prototyping and Manufacturing*, Paris, (2001).
20. G. Soler-Illia, C. Sanchez, B. Lebeau, and J. Patarin, ''Chemical Strategies to Design Textured Silica and Metal Oxide-Based Organised Networks: From Nanostructured Networks to Hierarchical Structures,'' Chem. Rev., 102, (2002), 4093–38
21. C. Sanchez, G. Soler-Illia, F. Ribot, and D. Grosso, ''Design of Functional Nanostructured Materials Through the Use of Controlled Hybrid Organic-Inorganic Interfaces,'' C.-R. Acad. Sci. Chim., 8, (2003), 109.
22. D. Grosso, F. Cagnol, G. J. de Soler-Illia, E. L. Crepaldi, H. Amenitsch, A. Brunet-Bruneau, A. Bourgeois, and C. Sanchez, ''Fundamentals of Mesostructuring through Evaporation-Induced Self-Assembly,'' Funct. Mater., 14 [4] (2004), 309–22.
23. F. Cagnol, D. Grosso, G. J. A. A. Soler-Illia, E. L. Crepaldi, H. Amenitsch, and C. Sanchez, ''Humidity-Controlled Mesostructuration in CTAB Templated Silica Thin Films Processing,'' J. Mater. Chem., 13, (2002), 61.
24. G. J. A. A. Soler-Illia, E. L. Crepaldi, D. Grosso, D. Durand, and C. Sanchez, ''Structural Control in Self-Standing Mesostructured Silica Oriented Membranes and Xerogels,'' Chem. Commun., (2002), 2298.
25. C. Sanchez, B. Julian, P. Belleville, and M. Popall, ''Applications of Hybrid Organic–Inorganic NanocompositesMaterials,'' J. Mater. Chem., 15, (2005), 3559.
26. H. Fan, G. P. Lopez, and C. J. Brinker, ''Rapid Prototyping of Patterned Multifunctional Nanostructures,'' Mater. Res. Soc. Symp. Proc., 624, (2000), 231–40.
27. H. Fang, Y. Lu, A. Stump, S. T. Reed, T. Baer, R. Schunk, V. Perez-Luna, G. P. Lopez, and C. J. Brinker, ''Rapid Prototyping of Patterned Functional Nanostructures,'' Lett. Nat., 405, (2001),56–9.
28. H. Fang, S. Reed, T. Baer, R. Schunk, G. P. Lopez, and C. J. Brinker, ''Hierarchically Structured Functional Porous Silica and Composite Produced by Evaporation-Induced Self-Assembly,'' Micropor. and Mesopor. Mater., 44–45, (2001), 625–37.
29. M. Lejeune, R. Noguera and T. Chartier. 3D fine scale ceramic components formed by ink-jet prototyping process. *J. Eur. Ceram. Soc.* **25** [12] (2005), 2055-2059.
30. M. Mougenot, M. Lejeune, J.F. Baumard, C. Boisière, F. Ribot, D. Grosso, C. Sanchez, ''Ink Jet Printing Arrays of Mesostructured Silica'', J. Am. Ceram. Soc., **89** [6] (2006), 1876-1882.
31. W.A. Smith and B. A. Auld. "Modeling 1-3 composite Piezoelectrics: Thickness-Mode Oscillations", IEEE. Trans. Ultrason. Ferroelectr. Freq. Control. 38[1] (1991), 40-47.
32. D. Grosso, A. Balkenende, P.A. Albouy, A. Ayral, H. Amenitsch, F. Babonneau, ''Two-Dimensional Hexagonal Mesoporous Silica Thin Films Prepared from Block Copolymers : Detailed Characterization and Formation Mechanism'', Chem. Mater., 13, (2001), 1848-1856
33. D. Grosso, F. Babonneau, C. Sanchez, J. Galo, E. Crepaldi, "A first insight in the mechanisms involved in the self-assembly of 2D hexagonal templated SiO2 and TiO2 mesostructured films during dip-coating", Journal of sol-gel science and technology, 26, (2003) 561-565
34. M. Klotz, P.A. Albouy, A. Ayral, C. Ménager, D. Grosso, A. Van der Lee, V. Cabuil, F. Babonneau, C. Guizard, "The true structure of hexagonal mesophase-templated silica films as revealed by X-Ray scaterring : Effects of thermal treatments and of nanoparticle seeding", Chem. Mater., 12, (2000) 1721-1728.